ACS APPLIED MATERIALS & INTERFACES

Research Article

www.acsami.org

Cost-Effective Reduced Graphene Oxide-Coated Polyurethane Sponge As a Highly Efficient and Reusable Oil-Absorbent

Yue Liu,[†] Junkui Ma,[†] Tao Wu,[†] Xingrui Wang,[†] Guanbo Huang,[†] Yu Liu,[†] Haixia Qiu,[†] Yi Li,*[,†] Wei Wang,[‡] and Jianping Gao*[,†]

[†]School of Science and [‡]School of Chemical Engineering & Technology, Tianjin University, Tianjin 300072, P. R. China

Supporting Information

ABSTRACT: Reduced graphene oxide coated polyurethane (rGPU) sponges were fabricated by a facile method. The structure and properties of these rGPU sponges were characterized by Fourier transform infrared spectroscopy, thermal gravimetric analysis, X-ray diffraction, and scanning electron microscopy. The rGPU sponges are hydrophobic and oleophilic and show extremely high absorption for organic liquids. For all the organic liquids tested, the absorption capacities were higher than 80 g g^{-1} and 160 g g^{-1} (the highest value) was achieved for chloroform. In addition, the absorption capacity of the rGPU sponge did not deteriorate after it was reused 50 times, so the rGPU sponge has excellent recyclability.

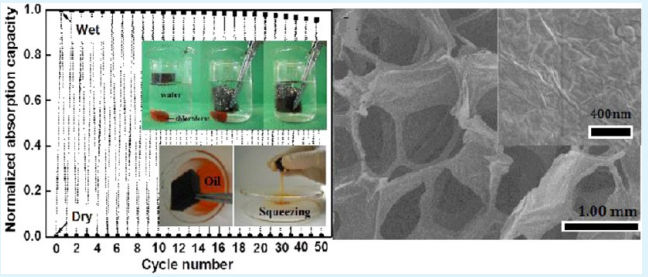

KEYWORDS: *reduced graphene oxide, polyurethane sponge, hydrophobic, oleophilic, oil absorption, recyclability*

1. INTRODUCTION

In recent years, oil spills and chemical leakage from industrial accidents have had catastrophic effects on marine and aquatic ecosystems.[1] Not only have numerous sea birds and mammals been killed but seaweed has also sustained serious damage. Therefore, the removal or collection of organic pollutants from water surfaces has attracted worldwide attention. Traditionally, oil spills are cleaned by a variety of methods, such as in situ burning,[2] mechanical collection,[3] chemical dispersants,[4] bioremediation,[5] and using absorbent materials.[6−8]

Because of their low operational costs and their ability to remove and collect oil, absorbent materials including zeolites,[8,9] activated carbon,[8] organoclays,[7,9] straw,[6,9] and wool fibers,[8] polypropylene fiber and alkyl acrylate copolymers[10] are considered desirable choices for the cleanup of oil spills.[11] Although widely used in practical applications, these absorbent materials still have limitations such as environmental incompatibilities, low absorption capacities and poor recyclabilities.[12] In particular, most of these materials absorb not only oils but also water, which reduces the separation selectivity and efficiency.[13] Therefore, an ideal absorbent material should have properties like a high oil absorption capacity, a high selectivity, a low density, excellent recyclability and environmental friendliness.[11]

Recently, materials with super-oleophilic properties have attracted considerable interest in the field of oil-water separation.[14,15] Carbon nanotubes,[16] mesh films,[17] filter paper,[18] and graphene[19] have all been used for separating oil from water. However, these materials have limitations for practical applications such as high costs, complex preparation processes, and difficulties in fabrication.

Polyurethane (PU) sponge is a kind of commercially available 3D porous material.[20] With high absorption abilities, low densities, and good elasticities, commercially available PU sponge provide excellent substrates for the fabrication of oil absorbents.[11] However, it is usually hydrophilic, which makes it impractical for the selective and efficient removal of oils from water. Therefore, modifications are needed to change them from hydrophilic to hydrophobic.

Graphene oxide (GO) is an oxygen-abundant material produced by the controlled oxidation of graphite.[21] It has an extended layered structure with hydrophilic polar groups (hydroxy, carboxyl and epoxy groups) protruding from its layers, which results in interesting swelling, intercalating and ion exchange properties.[22] Due to its low-cost, chemical stability, as well as its environmentally friendly properties, GO has aroused a great deal of interest in recent years.[23] Although GO is hydrophilic, the reduction of GO (to form reduced GO, rGO) changes the material from hydrophilic to hydrophobic because some of the polar functional groups on the GO are removed during the reduction process.[24]

Herein, an oil absorbent based on polyurethane sponges coated with rGO was fabricated by a facile method. The sponges were coated with a thin coating of rGO to obtain reduced graphene oxide coated polyurethane (rGPU) sponges which were then used to absorb different kinds of organic liquids (diesel oil, pump oil, lubricate oil, olive oil, bean oil, chloroform, toluene, tetrahydrofuran (THF), *N*,*N*′-dimethyl formamide (DMF) and dimethyl sulfoxide (DMSO)). The

Received: June 21, 2013
Accepted: September 19, 2013
Published: September 19, 2013

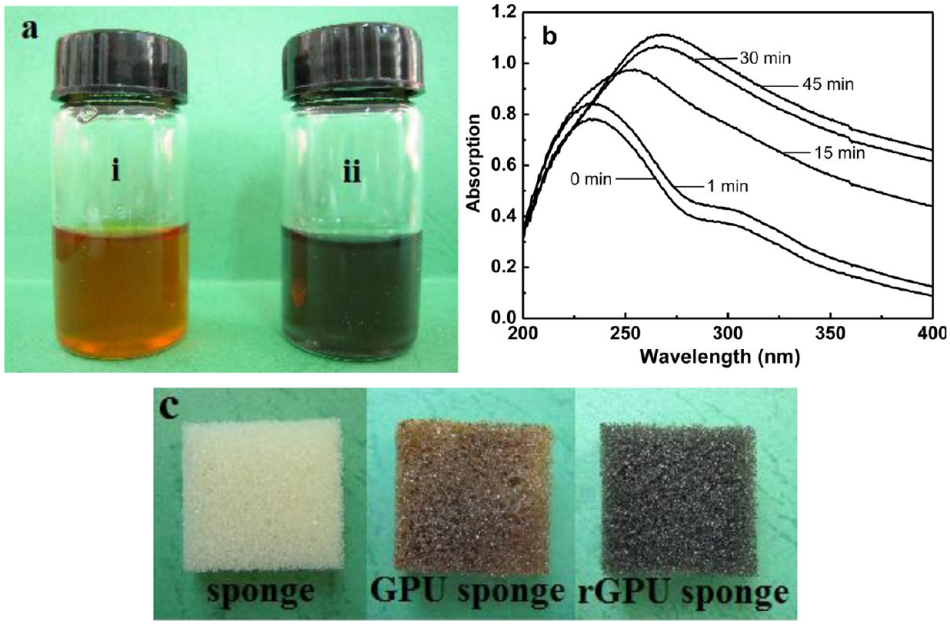

Figure 1. (a) Photographs of the aqueous suspensions of GO (1 mg mL^{-1}) (i) and RGO (ii), (b) UV−vis absorption spectra of the rGO suspension at different reduction times, and (c) photographs of the PU, GPU, and rGPU sponges.

coating of rGO not only makes the rGPU sponges hydrophobic but also increase their compressive strength. Therefore, a combination of high hydrophobicity, elasticity, and strength makes the rGPU sponge be a high efficient and reusable absorbent for spilling oil.

2. MATERIALS AND EXPERIMENTAL SECTION

2.1. Materials. Graphite was obtained from Huadong Graphite Co and the polyurethane sponges were from Shanghai Foam Materials Co. Chloroform, acetone, THF, DMF, DMSO, and hydrazine were all from Tianjin Chemical Reagent Co. All the chemicals were used as received.

2.2. Preparation of GO. GO was prepared from purified natural graphite by a modified Hummer's method.[25] Briefly, concentrated H_2SO_4 was added into a 250-mL flask filled with graphite, followed by the addition of $NaNO_3$. Then solid $KMnO_4$ was gradually added with stirring while the temperature of the mixture was kept below 20 °C. Next the temperature was increased to 30 °C and excess distilled water was added to the mixture and the temperature was then increased to 80 °C. Finally, 30% H_2O_2 was added until the color of mixture changed to brilliant yellow. The mixture was filtered and washed several times with 5% aqueous HCl to remove metal ions and then washed with distilled water to remove the acid. The resulting filter cake was dried in air then redispersed into water. Suspended GO sheets were obtained after ultrasonic treatment.

2.3. Preparation of Graphene Oxide-Coated Polyurethane (GPU) sponges and rGPU Sponges. The polyurethane sponge was cut into blocks and ultrasonically cleaned in ethanol. Then the blocks were rinsed with distilled water and dried at 60 °C in an oven. The sponge blocks were then immersed in a GO suspension (2 mg mL^{-1}) for 1 h and then taken out and washed with copious amounts of distilled water. They were then put in a vacuum oven and dried for 24 h at 30 °C to obtain the GPU sponge.

To preparation the rGPU sponges, the treated polyurethane sponge blocks were immersed in the GO suspension (2 mg mL^{-1}) for 1 h. Then the pH of the solution was adjusted to 9 using ammonia before the GO was subjected to reduction by hydrazine at 80 °C for 1 h.[26,27] During this time the extent of GO reduction was monitored with a UV-Vis spectrophotometer (TU-1901, Matsushita Electric Japan). The sponge blocks were then taken out, washed with distilled water, and dried for about 24 h at 30 °C in a vacuum oven to obtain the rGPU sponges.

2.4. Characterization of the rGPU Sponges. *Physical Properties of the rGPU Sponges.* The density ρ of the sponge was calculated using the equation: $\rho = m/V$, where, m is the weight of the sponge and V is the volume of the sponge. The porosity of ϕ the sponge was calculated using the relationship: $\phi = 100(1 - (\rho/(\rho_s x + \rho_R y)))$, where, ρ, ρ_s and ρ_R are the densities of the sponge, polyurethane and rGO respectively and x and y are the weight percentages of the polyurethane sponge and the rGO respectively.

The hydrophobicity of the rGPU sponge was measured with an optical contact angle measuring device (OCA20110524; Dataphysics Instruments, Germany) using a droplet (4.8 μL) of water or lubricate oil as the indicator.

The compressive strength of the rGPU sponge was measured by placing the samples into a programmable temperature and humidity chamber with a temperature of 25 ± 2 °C and a relative humidity of 65 ± 2% for about 24 h. Then the compressive strengths of the samples were measured with a dynamic mechanical analyzer at a compressing rate of 1 mm/min.

Scanning Electron Microscopy (SEM) Observation of the rGPU Sponges. The porous structure of the rGPU sponges was observed with a scanning electron microscope (JEOL-6700F ESEM, Japan). Before observation, the samples were coated with gold using a sputtering coater (Desk-II; Denton Vacuum, Japan).

Fourier Transform Infrared (FT-IR) Spectra of the rGPU Sponges. A Fourier transform infrared spectrometer (Paragon-1000, Perkin-Elmer, USA) was used to confirm the deposition of rGO on the walls of polyurethane sponge. The spectra were obtained in the range of 500−4000 cm^{-1} by averaging 16 scans at a resolution of 4 cm^{-1} at 1 min intervals to minimize the effects of dynamic scanning.

X-ray Photoelectron Spectra (XPS) of GO and rGO. The elemental composition analyses of GO and rGO were determined using X-ray photoelectron spectroscopy (PHI1600 ESCA System, PERKIN ELMER, USA) with Al Ka radiation ($h\nu$ = 1486.6 eV). The XPS were fitted using the XPS peak 4.1 software in which a Shirley background was used to perform curve fitting and to calculate the atomic concentrations.

X-ray Diffraction (XRD) of the rGPU Sponges. The X-ray diffraction diagrams of the samples were measured on a X'pert, PANAlytical X-ray diffractometer using Cu Kα radiation (λ = 1.73 Å) at a scanning rate of 4°/min with a voltage of 45 kV and a current of

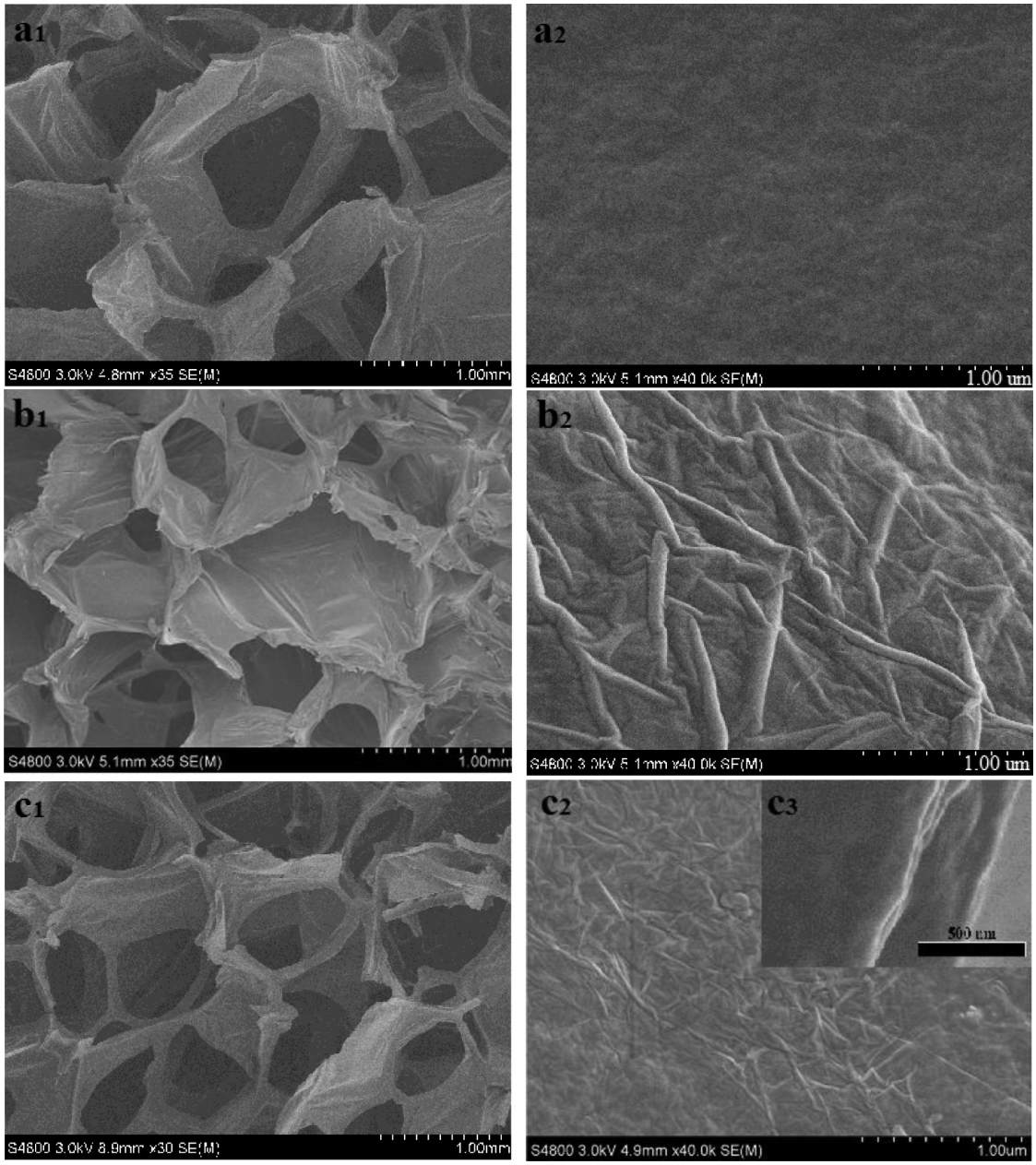

Figure 2. SEM photos of a (a_1, a_2) PU sponge, (b_1, b_2) GPU sponge, and (c_1, c_2, c_3) rGPU sponge.

30 mA. The data were collected from 10 to 30° (2θ) with a step of 0.0037° and a measuring time of 5 s/step.

Thermogravimetric Analysis (TGA) and Differential Thermal Gravity (DTG) of the rGPU Sponges. The samples were dried to a constant weight in a vacuum at 30 °C, and then the thermogravimetric diagrams of the samples were measured using a heating rate of 6 °C min^{-1} (Rigaku-TD-TDA, Japan).

2.5. Absorption of the rGPU Sponges for Organic Liquids. The absorption capacities (Q) of the rGPU sponges for various organic liquids (including lubricate oil, olive oil, bean oil, diesel oil, pump oil, chloroform, acetone, THF, DMF and DMSO) were measured. A weighed amount of rGPU sponge was put into a 200-mL conical flask containing 40 mL of organic liquid and allowed to absorb at room temperature for 5 min. Then the soaked rGPU sponge was removed and its weight was measured. The Q was calculated with the equation: $Q = (m_e - m_0)/m_0$, where, m_0 and m_e are the sponge weights before and after the absorption test, respectively.

3. RESULTS AND DISCUSSION

3.1. Characterization of the GPU and rGPU Sponges. The GO was prepared from purified natural graphite in our laboratory by a modified Hummer's method.[25] The graphite oxide was rinsed and centrifuged eight times to remove residual salts and acids, and then a stably dispersed GO aqueous suspension was prepared via ultrasonication. The GO has previously been characterized by transmission electron microscopy, X-ray photoelectron spectroscopy analysis, and Raman spectroscopy.[28] These analyses confirm that the GO is made up of a single or a few layers and contains many oxygen-containing groups. The stable GO aqueous suspension can be used in applications, including the reduction of GO to prepare rGO.

The GPU and rGPU sponges were fabricated by coating PU sponges with GO or RGO respectively. The GPU sponge was formed by immersing a PU sponge block in a GO suspension

for 1 h. After immersion the sponge was washed with copious amounts of distilled water. The rGPU sponge was formed after the GPU sponge was subjected to reduction by hydrazine at 80 °C for 1 h.

Figure 1 shows the changes in color and the UV−vis spectra of the GO suspension that was reduced by hydrazine at 80 °C. The red shift of the absorption peak maximum (λ_{max}) has been used to determine the extent of GO reduction in many papers that have studied the reduction of GO by new reductants.[29] The GO suspension quickly changed from yellow to black and the λ_{max} of the GO suspension at 226 nm gradually red shifted to 268 nm after 45 min of reaction (Figure 1b). This suggests that the GO was reduced, and the electronic conjugation within the RGO nanosheets was restored.[30] Longer reduction times did not result in any further peak shift. So the GPU sponge was reduced by hydrazine for 1 h at 80 °C to produce an rGPU sponge. Like the GO suspension, the GPU sponge changed from brown to light black after reduction (Figure 1c). To further examine the extent of reduction in rGO, XPS of GO and rGO was performed and the results are shown in Figure S1 in the Supporting Information. After reduction, the C/O ratio increased from 2.6 to 9.1, which indicates an effective reduction of GO.

The porous structure of the PU, GPU and rGPU sponges was observed by SEM and the photos are shown in Figure 2. They have almost the same porous structure, which indicates that GO and rGO coatings did not influence the porous structure of the PU sponge. However the morphologies of the wall surfaces of the GPU (Figure $2b_2$) and rGPU sponges (Figure $2c_2$) are completely different from that of the PU sponge. They are full of wrinkles whereas the surface of the PU sponge (Figure $2a_2$) is smooth. These wrinkles are probably caused by thin coatings of GO and rGO, which are about 10 nm according to Figure $2c_3$. These results confirm that the GO and rGO coatings are uniformly deposited on the surfaces of the pores of the PU sponges.

Typical FT-IR spectra of GO, rGO, the PU sponge, the GPU sponge, and the rGPU sponge are shown in Figure 3. The

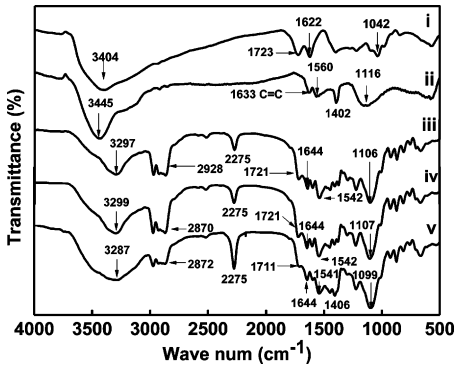

Figure 3. FT-IR spectra of GO (i), rGO (ii), PU sponge (iii), GPU sponge (iv), and rGPU sponge (v).

strong peaks at 3404, 1725, 1402, 1224, and 1042 cm^{-1} in the GO spectrum are associated with O−H stretching, C═O stretching, OH deformation, epoxy C−O stretching, and alkoxy C−O stretching, respectively.[31,32] In the rGO spectrum, the peak at 1725 cm^{-1} is not present, whereas the peak at 1625 cm^{-1} has increased in intensity, which indicates that most of the oxygen groups were removed during the transformation from GO to rGO.

For the PU sponge, the stretching vibration of N−H occurs at 3297 cm^{-1}. The peak at 2928 cm^{-1} is due to the C−H stretching of $-CH_3$ and $-CH_2$, and the peak at 2275 cm^{-1} is due to the asymmetric stretching of −NCO. The peaks at 1721, 1644, and 1106 cm^{-1} are associated with C═O stretching in the amide, urea and ether groups respectively, and the peak at 1542 cm^{-1} is attributed to the amide II band. Most of characteristic peaks of PU, GO and rGO between 1000 and 1800 cm^{-1} are similar.

For GPU and rGPU sponges, the peak at about 3290 cm^{-1} broadens and increases in intensity compared to GO and RGO which may be due to an overlap of the O−H and N−H stretching vibrations. The peaks at 2870 and 2275 cm^{-1} are attributed to C−H stretching and −NCO asymmetric stretching respectively. The above IR spectra indicate that no new bonds were formed in the GPU and rGPU sponges.

To get information about the crystalline structure of the sponges, we measured XRD patterns of GO, rGO, PU, rGPU, and GPU sponges and are shown in the Figure 4. GO shows a

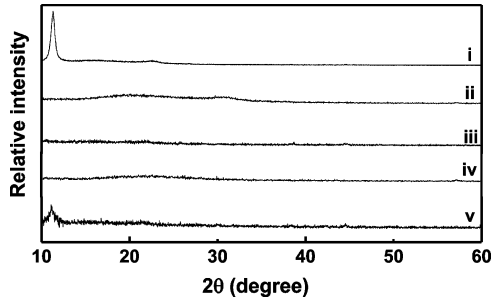

Figure 4. XRD spectra of the (i) GO, (ii) rGO, (iii) PU sponge, (iv) rGPU sponge, and (v) GPU sponge.

characteristic diffraction peak at 11.4°, which indicates the interlayer spacing of the graphene oxide was about 0.80 nm. This indicates that the GO retains a layered structure. The large interlayer distance is attributed to the formation of hydroxyl, epoxy and carboxyl groups which causes the intercalation of water molecules and increases the distance between the layers. However, this peak disappears in the XRD pattern of rGO which can be attributed to the successful reduction of the GO. The PU sponge has no characteristic diffraction peaks because it is amorphous. The GPU sponge shows a characteristic diffraction peak at 11.4° like GO, indicating that the PU sponge has been coated with GO. The XRD diagrams of rGO and the rGPU sponge are similar indicating that the GO coating on the GPU has been reduced to rGO.

Thermo gravimetric analysis is a standard technique to determine the composition or thermal stability of materials. Here, it was performed to determine the effect of the GO or rGO coating on the thermal decomposition behavior of the PU sponge. The TGA curves of rGO and the PU and rGPU sponges are shown in Figure 5. The TGA curves of the PU and rGPU sponges are similar and both have a rapid weight loss in the temperature range of 250−400 °C. Figure S2 shows the DTG curves of rGO, a PU sponge and an rGPU sponge. The peak temperature (T_p) of the DTG curves represents the temperature at which the maximum weight loss rate was reached. The T_p of the PU sponge and the rGPU sponge are similar. These indicate that the amount of rGO coated on the rGPU sponge is too small to affect the decomposition behavior of the PU sponge. However, the total weight loss of the PU

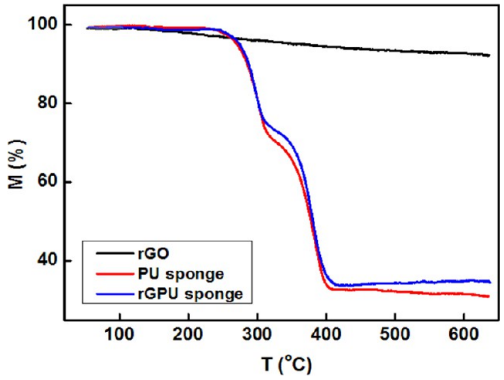

Figure 5. TGA curves of the rGO, PU sponge and rGPU sponge.

sponge is slightly higher than that of the rGPU sponge. Under a nitrogen atmosphere, the residual weight should be related to the amount of carbon in the samples, which is 92.7% for rGO, 30.5% for the PU sponge, and 33.6% for the rGO-sponge. On the basis of these results, the weight percent of rGO in the rGPU sponge was about 4.9%.

3.2. Absorption Capacity of the rGPU Sponges for Organic Liquids. The above analyses have proven that GO and rGO can be easily coated on the surfaces of the pores in PU sponges to form GPU and rGPU sponges. These sponges are light and elastic. They deform under pressure and recovery quickly after the pressure is released. These physical properties are usually required for absorbents. Table 1 gives the densities

Table 1. Density and Porosity of the PU, GPU, and rGPU Sponges

samples	ρ (g cm^{-3})	ϕ (vol %)
PU sponge	0.0085	99.30
GPU sponge	0.0090	99.28
rGPU sponge	0.0088	99.29

and porosities of the sponges. The density and porosity of the PU sponge are 0.0085 g cm^{-3} and 99.30 vol %, respectively, and those of rGPU sponge are 0.0088 cm^{-3} and 99.29 vol %, respectively. So the rGO coating does not obviously change the porosity of the PU sponge.

To determine the hydrophobicity or oleophilicity of the rGPU sponge, its contact angle was measured. As shown in Figure 6, (a) the water contact angle of the prepared sponges was 127°, whereas (b) a drop of lubricating oil completely spread out and was infused into the pores of the rGPU sponge within one second and so no contact angle could be measured. These phenomena indicate that the rGPU sponge is oleophilic. The high porosity and oleophilicity make rGPU sponge a good absorbent for oil.

Figure 6c shows the compressive strengths of the PU and rGPU sponges. The compressive strength was measured when the sponge volume had decreased by 40%, and this measurement was repeated 400 times. The compressive strength of the rGPU sponge is obviously higher than that of PU sponge. For both sponges, the compressive strength decreased with the number of measurements although the strength for the PU sponge reduced more rapidly than that for the rGPU sponge. The inset photos in Figure 6c proven good recovery of the elasticity in the process of repeated compression. In summary, the rGO coating increases the compressive strength of the PU sponge, but does not affect the elasticity.

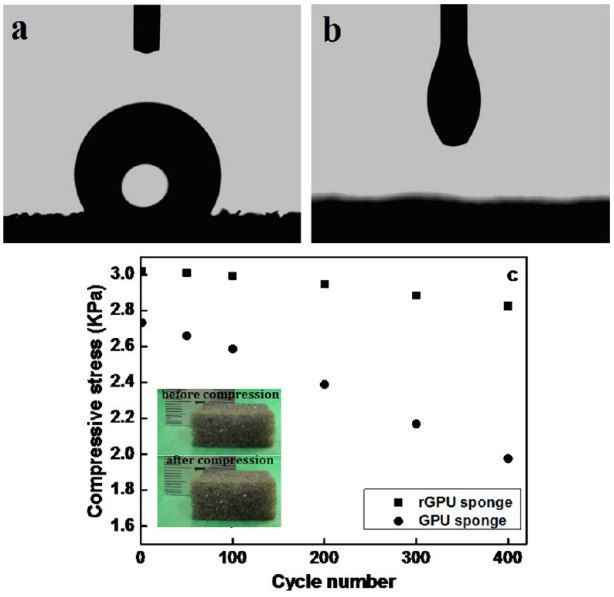

Figure 6. Optical images of a water droplet (a) and a lubricating oil droplet (b) placed on the rGPU sponge. (c) Compressive strengths and photographs of the rGPU sponge before and after repeated compression.

The above results show that the rGPU sponge is highly porous and oleophilic. The porous structure should result in a high absorbance for liquids, whereas the super-hydrophobicity and super-oleophilicity should give a good oil/water separation capacity. When a rGPU sponge was placed on a diesel oil (dyed with Sudan I)-water mixture (Figure 7a), the rGPU sponge quickly and selectively absorbed the diesel oil from the mixture and left a clear ring around the sponge (Figure 7b).The oil-filled rGPU sponge then floated on the water (Figure 7c), which facilitated its easy collection. It usually only took a few minutes to complete the absorption.

As shown in Figure 7d–g, the rGPU sponge also effectively absorbed a high-density organic solvent (chloroform) from water. When a piece of rGPU sponge was forced into contact with chloroform in water, the chloroform was quickly sucked into the rGPU sponge within a few seconds. This makes the rGPU sponge a promising candidate for absorbing and eliminating high-density organic solvents in water.

To investigate the absorption capacities of the GPU and the rGPU sponges, several organic liquids were tested and the results are shown in Figure 8. It only took 20 s for the rGPU sponge immersed in oil to begin to sink and after 40s in oil the sponge was resting on the bottom of the beaker (Figure 8b). In contrast, if no external force was applied, the PU sponge was still floating on the surface of the oil after 24 h (Figure 8b), This difference is because the rGO coating increased the olephilicity of the sponge.

The data in Figure 8a shows that the Q values for the rGPU sponge for all the organic liquids tested were over 80 g g^{-1} and reached a maximum of 160 of g g^{-1} for chloroform. This is an extraordinary high value. The Q values for the GPU sponges varied from 70 to 140 g g^{-1}. As expected, for each of the organic liquids, the Q value of the GPU sponge was lower than that of the rGPU sponge, although the values are still higher than those for most of the other absorbents shown in Table 2. There are probably two reasons for the differences in Q values. First, the porosity of the rGPU sponge is higher than that of the

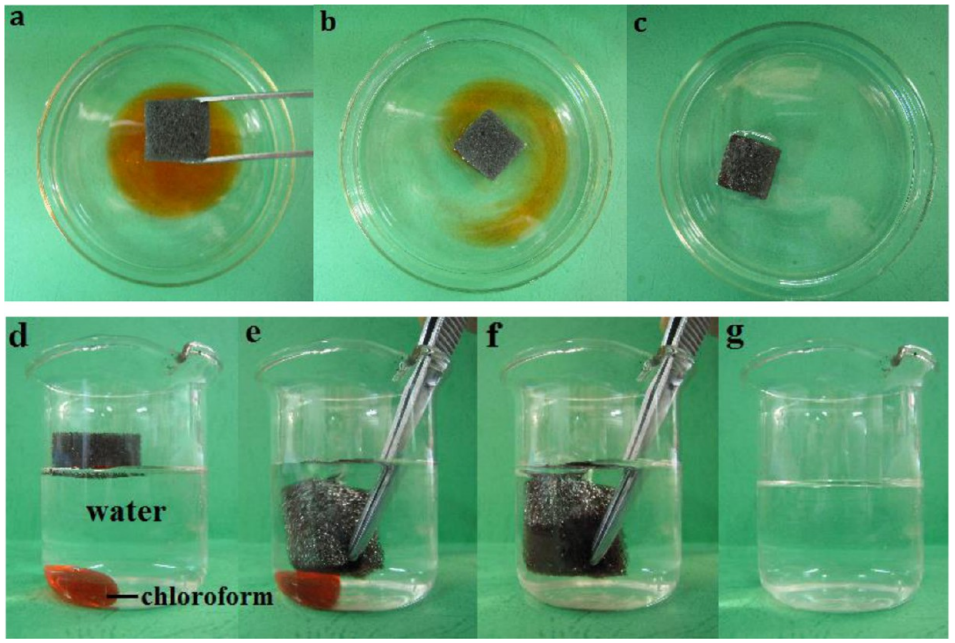

Figure 7. (a–c) Selective absorption of diesel oil (dyed with Sudan I) on water by the rGPU sponge and (d–g) selective absorption of chloroform (dyed with Sudan III) in water by the rGPU sponge.

GPU sponge (Table 1). Secondly, the rGPU sponge has fewer polar functional groups and is oleophilic, so it has a stronger affinity for organic liquid, which results in a higher absorption capacity.[33]

For both the GPU and rGPU sponges, the Q values for the various organic liquids are in the same order: chloroform (1.48 g cm^{-3}) > lubricate oil (0.96 g cm^{-3}) > pump oil (0.95 g cm^{-3}) >THF (0.89 g cm^{-3}) > DMSO (1.10 g cm^{-3}) > olive oil (0.90 g cm^{-3}) > bean oil (0.90 g cm^{-3}) > diesel oil (0.83 g cm^{-3}) > DMF (0.94 g cm^{-3}) > acetone (0.78 g cm^{-3}). It has been reported that the absorption capacity depends on the density of the organic liquid.[19] For example, the absorption capacities of a graphene sponge and a carbonaceous nanofiber aerogel are linearly related to the density of the organic liquid.[19,34] Absorption is based on the void volume in these porous materials. When the void volume is fixed, the volume occupied by the oil is also fixed. Therefore the absorption capacity is linearly related to the oil density.

However GPU and rGPU sponges do not follow this rule. For instance, the Q for THF is higher than that for DMSO even though the density of THF (0.89 g cm^{-3}) is lower than that of DMSO (1.10 g cm^{-3}). This may be attributed to the swelling of the PU sponge in organic liquids. It is speculated that the extent of swelling of the PU sponge in THF is larger than that in DMSO. The effect of the swelling on the Q is most obvious in chloroform. The GPU and rGPU sponges showed extraordinary high Q values in chloroform because their volume increased greatly because of swelling. Once the oil was squeezed out, they returned to their original volumes.

The absorption rates of the rGPU sponge for all the oils are rapid ($\leq$ 100 s) and are related to the viscosity of the oils as shown in Figure 8c. For the organic solvents (chloroform, DMF, DMSO, THF, and acetone), the absorption rate was so fast that the absorption equilibrium time could not be recorded.

The recyclability of an absorbent and the recoverability of the absorbed oils and organic solvents are key requirements in practical oil cleanup applications.[33] The photos in Figure 9 show that the absorbed diesel oil in the rGPU sponge can be recovered by manually squeezing the PU sponge. To test the recyclability of the GPU and rGPU sponges as absorbents, we alternately immersed the sponges in diesel oil for absorption and then squeezed to release the oil.

As shown in Figure 9a, the absorption capacity of the rGPU sponge did not deteriorate, and the weight of the dry rGPU sponge did not change when the rGPU sponge was reused 50 times. The recyclability of the rGPU sponge is much better than those of most sorbents, including the graphene-based sorbent reported by Nguyen et al.[43] The graphene-based sorbent has a high absorption capacity, but its recyclability is not good. For oils, the absorption capacities decreased to 20% of their initial value after the second cycle. This may be attributed to the weak adhesion between the graphene nanosheets and the sponge skeletons, although before use the graphene-based sorbent was modified by dipping into a dilute solution of polydienthylsiloxane to enhance the interfacial adhesion. However, the graphene coating was easily detached when the graphene-based sorbent was manual squeezed. The absorption capacity of the GPU sponge started to deteriorate after only 5 cycles (Figure 9b). This deterioration is due to the leaching of the GO from the GPU sponge, which is indicated by the color change of the used oil after several cycles. The above results show that the rGPU sponge not only has a high absorption capacity for organic liquids but also has excellent recyclability.

Table 2 lists the absorption capacity of previously reported absorbents. Obviously, the absorption capacities of the polymeric materials or natural inorganic materials are much lower than those of the carboneous materials. The graphene sponge (GS), graphene–carbon nanotube (CNT), hybrid foam and CNT sponge all had absorption capacities higher than 80 g g^{-1} with maximum values of 110 g g^{-1} for vegetable oil and 130 g g^{-1} for toluene. However, these absorbents exhibit poor recyclability.[19] The CNT sponge can be reused by squeezing, but its sorption capacity rapidly decreases to 20% of the initial

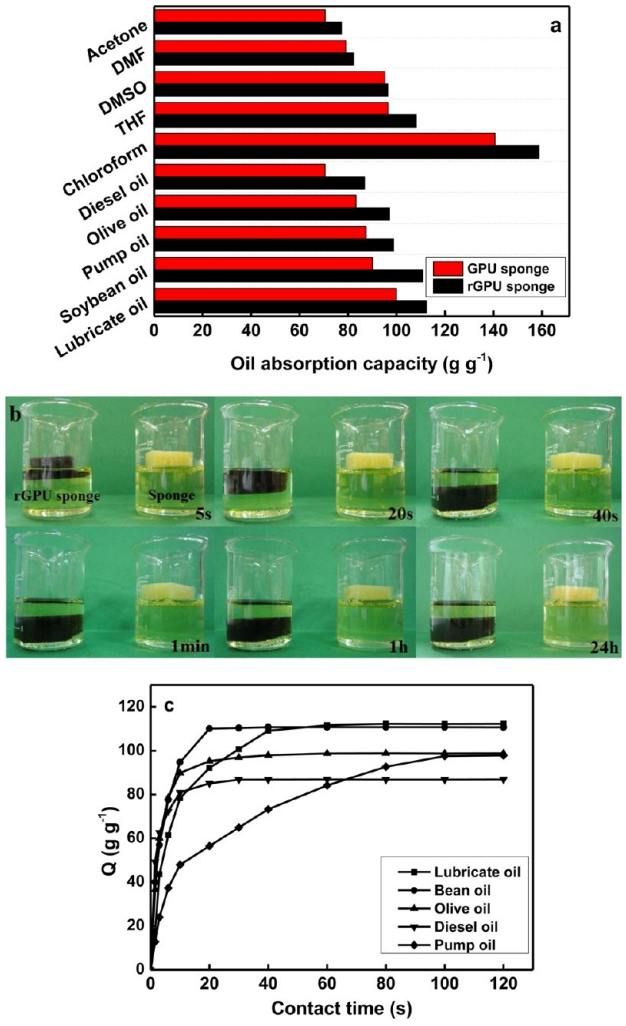

Figure 8. (a) Absorption capacity of the GPU and rGPU sponges for various organic liquids, (b) photos of the absorption processes for the PU and rGPU sponges, (c) absorption capacities of the rGPU sponge versus contact time with various oils.

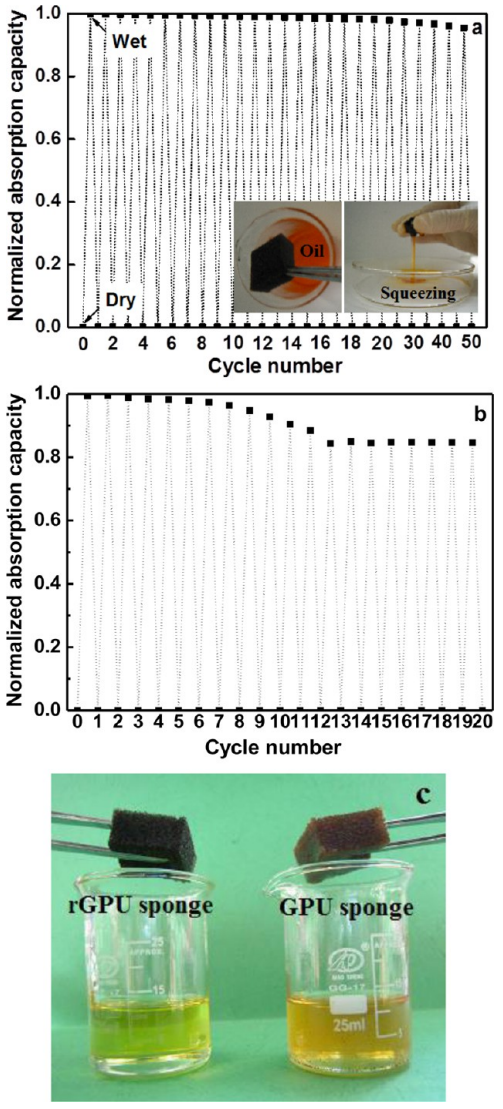

Figure 9. Recyclability of the (a) rGPU and (b) GPU sponge and (c) photos of the diesel oil after multiple cycles. The absorption capacity after multiple cycles is normalized by the initial weight gain.

value after the second cycle.[42] The GS and graphene−CNT hybrid foam cannot be squeezed because of low elasticity. They can, however, be reused after heat treatment (burning) but this is only feasible for organic solvents and it is an inefficient method.

The rGPU sponge not only has a high absorption capacity and recoverability, but it is also cost effective compared with graphene and carbon nanotube sponges which also have high absorption capacities. Therefore rGPU sponges are very

Table 2. Comparison of the Absorption Capacities of Various Materials

sorbent	oil	Q (g g^{-1})	solvent	Q (g g^{-1})	ref
sepiolite	motor oil	0.18			35
polydienthylsiloxane	motor oil	5	chloroform	11	23
corn stalk	gas oil	8			36
polypropylene	fuel oil	15.7	toluene	11.4	37
butyl rubber	crude oil	23	toluene	17.8	37
modified PU sponge	lubricate oil	25	dodecane	18	38
CNF[a]/carbon foam	wash oil	28.4			39
exfoliate graphite	heavy oil	75			40
graphene sponge	castor oil	75	chloroform	87	19
graphene−CNT[b] hybrid foam	sesame oil	105	toluene	130	41
CNT sponge	mineral oil	126	ethyl acetate	120	42

[a]Carbon nanofiber. [b]Carbon nanotube.

dx.doi.org/10.1021/am4024252 | ACS Appl. Mater. Interfaces 2013, 5, 10018−10026

promising potential absorbents for the treatment of oil spills or for oil-water separation.

4. CONCLUSIONS

A rGPU sponge was fabricated by coating a PU sponge with GO and then reducing the GO with hydrazine at 80 °C for 1 h. The prepared rGPU sponge has high compressive strength compared with the PU sponge. Because it is super-hydrophobic and super-oleophilic, the rGPU sponge showed high selectivity when it was employed as an absorption material for collecting organic solvents from water surfaces. The rGPU sponge had absorption capacities higher than 80 g g^{-1} for all the tested oils and achieved a maximum value of 160 g g^{-1} for chloroform, which is higher than most other absorbents. The Q values for the rGPU sponge for organic liquids is in the order: chloroform (1.48 g cm^{-3}) > lubricate oil (0.96 cm^{-3}) > pump oil (0.95 g cm^{-3}) >THF (0.89 g cm^{-3}) > DMSO (1.10 g cm^{-3}) > olive oil (0.90 cm^{-3}) > bean oil (0.90 cm^{-3}) > diesel oil (0.83 cm^{-3}) > DMF (0.94 g cm^{-3}) > acetone (0.78 g cm^{-3}). This order is not the same as the density order of the organic liquids. This phenomenon is attributed to the swelling of the PU sponge in organic solvents.

The absorption capacity of the rGPU sponge did not deteriorate, and the weight of the dry rGPU sponge did not change when the rGPU sponge was reused for 50 times. The rGPU sponge not only has a high absorption capacity for organic liquids, but also has excellent recyclability. Because the rGPU sponge is much more cost effective than graphene and carbon nanotube aerogels, it should be a very promising potential absorbent for the treatment of oil spills and for oil water separation.

■ ASSOCIATED CONTENT

Ⓢ Supporting Information

XPS spectra and analysis; differential thermal gravity curves (PDF). This material is available free of charge via the Internet at http://pubs.acs.org.

■ AUTHOR INFORMATION

Corresponding Authors

*E-mail: jianpingg@eyou.com.
*E-mail: liyi@tju.edu.cn.

Notes

The authors declare no competing financial interest.

■ ACKNOWLEDGMENTS

This work was supported by the National Science Foundation of China (21074089 and 21276181)

■ REFERENCES

(1) Calcagnile, P.; Fragouli, D.; Bayer, I. S.; Anyfantis, G. C.; Martiradonna, L.; Cozzoli, P. D.; Cingolani, R.; Athanassiou, A. *ACS Nano* **2012**, *6*, 5413−5419.
(2) Buist, I.; Potter, S.; Nedwed, T.; Mullin. *Cold Reg. Sci. Technol.* **2011**, *67*, 3−23.
(3) Keller, A. A.; Broje, V. *Environ. Sci. Technol.* **2006**, *40*, 7914−7918.
(4) Kujawinski, E. B.; Soule, M. C. K.; Valentine, D. L.; Boysen, A. K.; Longnecker, K.; Redmond, M. C. *Environ. Sci. Technol.* **2011**, *45*, 1298−1306.
(5) Aziz, H. A.; Zahed, M. A.; Isa, M. H.; Mohajeri, L.; Mohajeri, S. *Bioresour. Technol.* **2010**, *101*, 9455−9460.
(6) Choi, H. M.; Cloud, R. M. *Environ. Sci. Technol.* **1992**, *26*, 772−776.
(7) Adebajo, M. O.; Frost, R. L.; Kloprogge, J. T.; Carmody, O.; Kokot, S. *J. Porous Mater.* **2003**, *10*, 159−170.
(8) Bayat, A.; Aghamiri, S. F.; Moheb, A.; Vakili −Nezhaad, G. R. *Chem. Eng. Technol.* **2005**, *2*, 1525−1528.
(9) Radetic, M. M.; Jocic, D. M.; Jovancic, P. M.; Petrovic, Z. L.; Thomas, H. F. *Environ. Sci. Technol.* **2003**, *37*, 1008−1012.
(10) Lin, J. Y.; Ding, B.; Yang, J. M.; Yu, J. Y.; Sun, G. *Nanoscale* **2012**, *4*, 176−82.
(11) Chu, Y.; Pan, Q. M. *ACS Appl. Mater. Interface* **2012**, *4*, 2420−2425.
(12) Zhu, Q.; Pan, Q. M.; Liu, F. T. *J. Phys. Chem. C* **2011**, *115*, 17464−17470.
(13) Ceylan, D.; Dogu, S.; Karacik, B.; Yakan, S. D.; Okay, O. S.; Okay, O. *Environ. Sci. Technol.* **2009**, *43*, 3846−3852.
(14) Yao, X.; Song, Y. L.; Jiang, L. *Adv. Mater.* **2011**, *23*, 719−734.
(15) Yuan, J. K.; Liu, X. G.; Akbulut, O.; Hu, J. Q.; Suib, S. L.; Kong, J.; Stellacci, F. *Nat. Nanotechnol.* **2008**, *3*, 332−336.
(16) Gui, X. C.; Wei, J. Q.; Wang, K. L.; Cao, A. Y.; Zhu, H. W.; Jia, Y.; Shu, Q. K.; Wu, D. H. *Adv. Mater.* **2010**, *22*, 617−621.
(17) Feng, L.; Zhang, Z. Y.; Mai, Z. H.; Ma, Y. M.; Liu, B. Q.; Jiang, L.; Zhu, D. B. *Angew. Chem. Int. Ed.* **2004**, *43*, 2012−2014.
(18) Wang, S. H.; Li, M.; Lu, Q. H. *ACS Appl. Mater. Interface* **2010**, *2*, 677−683.
(19) Bi, H. C.; Xie, X.; Yin, K. B.; Zhou, Y. L.; Wan, S.; He, L. B.; Xu, F.; Banhart, F.; Sun, L.; Ruoff, R. S. *Adv. Funct. Mater.* **2012**, *21*, 4421−4425.
(20) Zhu, Q.; Chu, Y.; Wang, Z. K.; Chen, N.; Lin, L.; Liu, F. T.; Pan, Q. M. J. *Mater. Chem. A* **2013**, *1*, 5386−5393.
(21) Novoselov, K. S.; Geim, A. K.; Morozov, S. V.; Jiang, D.; Zhang, Y.; Dubong, S. V.; Grigorieva, I. V.; Firsov, A. A. *Science* **2004**, *306*, 666−669.
(22) Novoselov, K. S.; Geim, A. K.; Morozov, S. V.; Jiang, D.; Katsnelson, M. I.; Grigorieva, I. V.; Dubong, S. V.; Firsov, A. A. *Nature* **2005**, *438*, 197−200.
(23) Geim, A. K.; Novoselov, K. S. *Nat. Mater.* **2007**, *6*, 183−190.
(24) Marcano, D. C.; Kosynkin, D. V.; Berlin, J. M.; Sinitskii, A.; Sun, Z. Z.; Slesarev, A.; Alemany, L. B.; Lu, W.; Tour, J. M. *ACS Nano* **2010**, *4*, 4806−4814.
(25) Hummers, W.; Offeman, R. *J. Am. Chem. Soc.* **1958**, *80*, 1339−1339.
(26) Stankovich, S.; Piner, P. D.; Chen, X.; Wu, N.; Nguyen, S. T.; Ruoff, R. S. *J. Mater. Chem.* **2006**, *16*, 155−158.
(27) Stankovich, S.; Dikina, D. A.; Piner, R. D.; Kohlhaas, K. A.; Kleinhammes, A.; Jia, Y.; Wu, Y.; Nguyen, S. T.; Ruoff, R. S. *Carbon* **2007**, *45*, 1558−1565.
(28) Long, Y.; Zhang, C.; Wang, X.; Gao, J.; Wang, W.; Liu, Y. *J. Mater. Chem.* **2011**, *21*, 13934−13941.
(29) Ferńandez Merino, M. J.; Guardia, L.; Paredes, J. I.; Villar Rodil, S.; Solís Fernández, P.; Tascón, J. M. D. *J. Phys. Chem. C* **2010**, *114*, 6426−6432.
(30) Zhu, C. Z.; Guo, S. J.; Fang, Y. X.; Dong, S. J. *ACS Nano* **2010**, *4*, 2429−2437.
(31) Zhu, C.; Guo, S.; Fang, Y.; Dong, S. *ACS Nano* **2010**, *4*, 2429−2437.
(32) Bose, S.; Kuila, T.; Uddin, M. E.; Kim, N. H.; Lau, A. K. T.; Lee, J. H. *Polymer* **2010**, *51*, 5921−5928.
(33) Choi, S. J.; Kwon, T. H.; Im, H.; Moon, D. I.; Baek, D. J.; Seol, M. L.; Duarte, J. P.; Choi, Y. K. *ACS Appl. Mater. Interfaces* **2011**, *3*, 4552−4556.
(34) Liang, H.; Guan, Q.; Chen, L.; Zhu, Z.; Zhang, W.; Yu, S. *Angew. Chem., Int. Ed.* **2012**, *51*, 5101−5105.
(35) Rajaković-Ognjanović, V.; Aleksić, G.; Rahaković, L. *J. Hazard. Mater.* **2008**, *154*, 558−563.
(36) Husseien, M.; Amer, A. A.; El-Maghraby, A.; Hamedallah, N. *J. Anal. Appl. Pyrol.* **2009**, *86*, 360−363.
(37) Ceylan, D.; Doyu, S.; Karacik, B.; Yakan, S.; Okay, O.; Okay, O. *Environ. Sci. Technol.* **2009**, *43*, 3846−3852.

(38) Zhu, Q.; Chu, Y.; Wang, Z. K.; Chen, N.; Lin, L.; Liu, F. T.; Pan, Q. M. *J. Mater. Chem. A* **2013**, *1*, 5386−5393.
(39) Xiao, N.; Zhou, Y.; Ling, Z.; Qiu, J. S. *Carbon* **2013**, *59*, 530−536.
(40) Zheng, Y.; Wang, H.; Kang, F.; Wang, L.; Inagaki, M. *Carbon* **2004**, *42*, 2603−2067.
(41) Dong, X. C.; Chen, J.; Ma, Y. W.; Wang, J.; Chan-Park, M. B.; Liu, X. M.; Wang, L. H.; Huang, W.; Chen, P. *Chem. Commun.* **2012**, *48*, 10660−10662.
(42) Gui, X. C.; Li, H. B.; Wang, K. L.; Wei, J. Q.; Jia, Y.; Li, Z.; Fan, L. L.; Cao, A. Y.; Zhu, H. W.; Wu, D. H. *Acta Mater.* **2011**, *59*, 4798−4804.
(43) Nguyen, D. D.; Tai, N. H.; Lee, S. B.; Kuo, W. S. *Energy Environ. Sci.* **2012**, *5*, 7908−7912.